Atmos. Chem. Phys. Discuss., doi:10.5194/acp-2016-806, 2016
Manuscript under review for journal Atmos. Chem. Phys.
Published: 24 October 2016

Atmospheric Chemistry and Physics Discussions

Investigation of new particle formation at the summit of Mt. Tai, China

Ganglin Lv[1], Xiao Sui[1], Jianmin Chen[1,2*], Rohan Jayaratne[3], Abdelwahid Mellouki[1,4]

[1]School of Environmental Science and Engineering, Environment Research Institute, Shandong University, Jinan, Shandong 250100, China

[2]Shanghai Key Laboratory of Atmospheric Particle Pollution and Prevention (LAP3), Institute of Atmospheric Sciences, Fudan University, Shanghai 200433, China

[3]International Laboratory for Air Quality and Health, Science and Engineering Faculty, Queensland University of Technology, GPO Box 2434, Brisbane QLD 4001, Australia

[4]Institut de Combustion, Aérothermique, Réactivité et Environnement, CNRS, 45071 Orléans cedex 02, France

Correspondence to: Jianmin Chen (jmchen@fudan.edu.cn); Tel.: +86 53188363711; fax: +86 531 88361990

Abstract. To date very few field observations of new particle formation (NPF) have been carried out at the high-elevation mountain sites in China. Simultaneously measurements of particle size distributions, gas species, meteorological conditions and $PM_{2.5}$ were performed at the summit of Mt. Tai (1530 m ASL) from 25 July to 24 October 2014 (I), 21 September to 9 December 2014 (И) and 16 June to 7 August 2015 (III). The results showed that: i) 66 NPF events were observed during 164 days, corresponding to an occurrence frequency of 40 %. Formation rates, growth rates and condensation sinks were in the range of 1.10-57.43 cm^{-3} s^{-1}, 0.58-7.76 nm h^{-1} and 0.40×10^{-2}-6.32×10^{-2} s^{-1}, respectively, and Mt. Tai appeared to show the larger formation rate and smaller growth rate relative to other locations in China. The mean value of sulfur dioxide on NPF days was 46 % higher than that on non-NPF days, and a higher sulfur dioxide concentration could improve the possibility of rich precursors for NPF. ii) Sulfuric acid condensation contributed to 16.20 % of growth rate, and sulfuric acid proxy showed an obvious correlation with total particle concentration of 3-6 nm ($N_{3\text{-}6\ nm}$). iii) Low $PM_{2.5}$ was favourable for nucleation, and NPF days with limited higher $PM_{2.5}$ seemed to have larger growth rates which might be related to particles recombination in close sizes. Four NPF events were observed on haze episodes, which could be promoted by potential specific mechanisms or pollutants. iv) Particles formed via NPF on both clean and polluted days mainly contributed to Aiken mode eventually, and $PM_{2.5}$ variation was always in accordance with particle total volume concentration.

Keywords. New particle formation; Mountain observation; Sulfuric acid; $PM_{2.5}$; Haze

1 Introduction

Atmospheric aerosol particles play critical roles affecting global radiation balance and climate, directly through scattering and absorption of solar radiation, and indirectly through modifying cloud properties as potential cloud condensation nuclei (CCN) (Kuang et al., 2010). Aerosol particles are involved in several atmospheric chemistry processes such as enhanced haze and decreased visibility, and they harm human health by inhalation as well (Han, 2012). Previous researches showed

Atmos. Chem. Phys. Discuss., doi:10.5194/acp-2016-806, 2016
Manuscript under review for journal Atmos. Chem. Phys.
Published: 24 October 2016

Atmospheric Chemistry and Physics Discussions

that the nucleation of atmospheric gas-phase precursors and its subsequent growth to larger particles，namely new particle formation (NPF) process, were the largest source of atmospheric aerosol particles (Zhang et al., 2012). Field observations exhibited NPF typically increased particle number concentration of two to ten times (Gong et al., 2010). Model studies also revealed that NPF accounted for 5-50 % of CCN in the lower boundary layer (Spracklen et al., 2008). Better understanding the effects and processes of NPF could help to control atmospheric aerosol pollution in China.

Recent decades with the development of particle size distribution instruments, NPF events have been widely observed all around the world. The observation sites refer to northern-most sub-arctic, remote boreal forests, industrialized agricultural regions, high-iodine coastal environments, polluted urban areas et al. (Dal Maso et al., 2002), and frequency of NPF events varies a lot in different fields. Hallar et al. (2011) reported that NPF events in urban areas such as Pittsburgh et al. occurred on about 35-50 %, while remote background sites in Finland and Sweden only showed 2-27 %. Manninen et al. (2010) found that frequency of NPF ranged from 21 % to 57 % based on twelve field sites over Europe, and the amount of observed NPF days was closely related to the regional atmospheric conditions.

In the past decade, many campaigns and studies on NPF have been carried out in China. In 2004 Wiedensohler et al. (2004) first reported the observation of NPF events in China using a Twin Differential Mobility Particle Sizer (TDMPS), and then Liu et al. (2008) made the observation of rural/coastal NPF cases in XinKen site (Guangdong Province) in the same year. In 2005 Gao et al. (2009) investigated the suburban NPF in the Yangtze River delta using a Wide-range Particle Spectrometer (WPS), and after then NPF observations in urban/suburban/rural environment were widely conducted around China (An et al., 2015; Wang et al., 2011). However, field campaigns of NPF on mountains in China have been very few so far. Wang et al. (2014b) reported the NPF observation at Mt. Huang (493 m ASL) with WPS instrument from 15 August to 15 September 2011, while its results had significant limitation in instruments and seasonal variation. Multi-season observation and improved nanometer-scale instrument would be essential and valuable for NPF research in mountain environment.

NPF refers to nucleation and growth two processes that are probably decoupled under most atmospheric conditions (Kulmala, 2003). Researchers noted that sulfuric acid, ammonia, organic vapors, iodide species et al. in the atmosphere were involved in nucleation process in specific conditions, and gaseous sulfuric acid was the most critical candidate that participated in binary, ternary and ion induced nucleation (Boy et al., 2005; Wang et al., 2011; Zhang, 2010; Saunders et al., 2010; Allan et al., 2015). Nucleation rate could be the function of sulfuric acid concentration with a power dependency exponent, and the value of exponent varied a lot under different nucleation theories (Kulmala et al., 2006; Wang et al., 2011). Particle growth process was also related to gaseous sulfuric acid, and some studies showed that sulfuric acid condensation could explain about 10 % of newly particle growth and it mainly contributed to the early stage of growth (Meng et al., 2015; Smith et al., 2008; Setyan et al., 2014; Qi et al., 2004). Sulfur dioxide photochemical oxidation was the critical source for gaseous sulfuric acid, and NPF was indirectly related to the sulfur dioxide.

The particle formation and growth rates vary with field environments. Kulmala et al. (2004) reviewing a number of studies

Atmos. Chem. Phys. Discuss., doi:10.5194/acp-2016-806, 2016
Manuscript under review for journal Atmos. Chem. Phys.
Published: 24 October 2016

found that typical formation rate was in the range of 0.01-10 cm^{-3} s^{-1}, while in some urban areas it might be as high as 100 cm^{-3} s^{-1} and in coastal zones even got up to 10^4-10^5 cm^{-3} s^{-1}. Typical growth rate of newly formed particles ranged from 1 to 20 nm h^{-1}, and at some coastal areas it might be as high as 200 nm h^{-1}.

In this paper, we presented the Mt. Tai (1530 m ASL) cases on NPF research as the clean mountain-top environment. Mountain observations were scarce and valuable for NPF study in China, especially using the advanced few nanometer particle size distribution instruments. Based on simultaneous measurements of size distributions, meteorological conditions, gaseous species and $PM_{2.5}$ et al., three campaigns (25 July to 24 October 2014, 21 September to 9 December 2014 and 16 June to 7 August 2015) were carried out to explore the following questions: (1) what are the general characteristics of NPF events on Mt. Tai and how do ambient conditions affect NPF? (2) What's the contribution of gaseous sulfuric acid estimation on nucleation and growth processes? (3) How does $PM_{2.5}$ vary during NPF days, and what's the difference of particle behaviors in clean NPF day versus polluted NPF day as well as haze NPF day versus non-haze NPF day?

2 Methodology

2.1 Site description

The observation was conducted at the summit of Mt. Tai (36.16 °N, 117.6 °E, 1530 m ASL) which is located in the middle part of Shandong Province, China. The field site is near the peak of Mt. Tai which is one of the highest mountains near the East China Sea on the transport path of the Asian continental outflow (Li et al., 2011), and it is surrounded by dense vegetation and mountains with few anthropogenic pollution. City of Tai'an (population: 5,500,000) is located about 6 km away to the south and southeast of the sampling site horizontally.

2.2 Measurement techniques

Two types of size distribution instruments, namely neutral cluster and air ion spectrometer (NAIS) and wide-range particle spectrometer (WPS), two gas monitors (SO_2 and O_3), a instrument for mass concentration of $PM_{2.5}$ were used in this study. In addition, meteorological parameters including temperature (T), relative humidity (RH), wind speed (WS), wind direction (WD), visibility et al. were also automatically recorded.

NAIS is a multichannel nanometer aerosol instrument which can measure the distribution of ions (charged particles and cluster ions) of both polarities and aerosol particles. Its measurement range of ion distribution is equivalent to 0.8-40 nm and particle distribution is 2-40 nm. The instrument consists of two multichannel electrical mobility analyzer columns, one for each polarity. The aerosols are classified according to mobility and measured with an array of twenty-one electrometers per column. In this work, the total time of each measurement cycle was set as 5 min, namely particles 120 s, ions 120 s and offset 60 s.

WPS is a high-resolution aerosol spectrometer which combines a differential mobility analyzer (DMA), a condensation

Atmos. Chem. Phys. Discuss., doi:10.5194/acp-2016-806, 2016
Manuscript under review for journal Atmos. Chem. Phys.
Published: 24 October 2016

Atmospheric Chemistry and Physics Discussions

particle counter (CPC) and a laser light scattering (LPS). The diameter range is from 10 to 10,000 nm, and 48 channels were used in DMA and 24 channels were in LPS. In this work, one scan time of entire size range was set as 5 min.

Concentration of sulfur dioxide in the atmosphere was measured using a pulsed ultraviolet fluorescence analyzer (Model 43C, Thermo Electron Corporation-TEC), and ozone was measured using an ultraviolet photometric analyzer (Model 49C, TEC). Mass concentration of $PM_{2.5}$ was detected by a monitor utilizing a combination of beta attenuation and light scattering technology (Model 5030 SHARP Monitor, Thermo Fisher Scientific), and meteorological data were obtained from an automatic meteorological station (MILOS520, Vaisala, Finland).

2.3 Data analysis

2.3.1 Formation rate, growth rate and condensation sink

Analysis of particle size distribution data was for formation rate and growth rate calculation, and particle group of 3-20 nm was regarded as nucleation particles because of its neglecting for pre-existing particle influence and quickly growing out of averaging range. The formation rate can be expressed (Dal Maso et al., 2005):

$$J_{3\text{-}20} = \frac{dN_{3\text{-}20}}{dt} + F_{\text{CoagS}} + F_{\text{growth}} \quad (1)$$

where $dN_{3\text{-}20}/dt$ is the net increase rate of nucleation particles, F_{CoagS} is coagulation loss and F_{growth} is the loss of particles growing out of size range which could be neglected in our observation. The equation for F_{CoagS} is (Kulmala et al., 2001; Fuchs, 1964):

$$F_{\text{CoagS}} = \sum_i \text{CoagS}\,(Dp_i) \cdot N_i \quad (2)$$

Growth rate is determined by the maximum concentration method (Kulmala et al., 2012), and that is:

$$\text{GR} = \frac{\Delta D_{\text{m}}}{\Delta t} = \frac{D_{\text{m2}} - D_{\text{m1}}}{t_2 - t_1} \quad (3)$$

Condensation sink determines the rate of molecules condensing on the pre-existing aerosols, and it can be required (Kanawade et al., 2014):

$$\text{CS} = 2\pi D \sum_i \beta_{Mi}\, Dp_i\, N_i \quad (4)$$

2.3.2 Sulfuric acid proxy

Based on solar radiation and sulfur dioxide concentration, gas-phase sulfuric acid could be roughly estimated and the sulfuric acid proxy ($[H_2SO_4]$) is expressed (Mikkonen et al., 2011):

$$[H_2SO_4] = 1.86 \cdot 10^{-1} \cdot k \cdot [\text{SR}] \cdot [SO_2]^{0.5} \quad (5)$$

here k is temperature-dependent reaction rate constant, solar radiation gets from Hybrid Single Particle Lagrangian Integrated Trajectory (HYSPLIT) Model in Air Resources Laboratory and may have some error with actual value.

Atmos. Chem. Phys. Discuss., doi:10.5194/acp-2016-806, 2016
Manuscript under review for journal Atmos. Chem. Phys.
Published: 24 October 2016

Atmospheric Chemistry and Physics Discussions

With the above sulfuric acid proxy, particle growth rate limited by sulfuric acid condensation was calculated (Kulmala et al., 2001; Boy et al., 2005):

$$\frac{dDp}{dt} = \frac{m_v \cdot \beta_M \cdot D \cdot C}{Dp \cdot \rho} \quad (6)$$

3 Results and discussion

3.1 Classification and characteristics of NPF events

Basically, an NPF event could be defined as the distinct new nucleation mode particles burst for significant hours and subsequent growth to larger size over a period of time (Dal Maso et al., 2005; Hallar et al., 2011; Wang et al., 2014a; Xiao et al., 2015). For our Mt. Tai observation, neutral particles generally accounted for more than 95 % of the total particles and air ion discussion might be neglected in this paper.

During the 164 days valid observation, NPF events occurred on 66 days overall and it corresponded to the nucleation probability of 40 %. NPF events could be observed in each month, and frequent NPF occurrence was in campaign И which showed the frequency of 56 % (others were only 21 % by contrast). It could be interpreted that campaign I and III were in rainy and foggy season, and such wet condition seemed adverse to NPF. Table 1 listed the various calculated parameters of all NPF events, including net nucleation particle increase rate ($dN_{3\text{-}20}/dt$), formation rate ($J_{3\text{-}20}$), growth rate (GR), condensation sink (CS), mean sulfur dioxide value during nucleation process, sulfuric acid proxy at the beginning of nucleation particles enhancing, growth rate limited by sulfuric acid condensation (GR-C) and ratio of GR-C to GR (GR-C/GR). The minimum and maximum of each calculated parameter were marked in blue and red in Table 1, respectively. Besides, Table 2 summarized the mean, median, 25th percentile, 75th percentile, minimum and maximum of these parameters, and in Table 3 it also exhibited the characteristics comparison between Mt. Tai and some other typical recent researches in China. Detailed discussions for them were in follows.

The net increase rates on Mt. Tai were in the range of 0.96-48.52 cm^{-3} s^{-1} and formation rates were 1.10-57.43 cm^{-3} s^{-1}. Coagulation loss averagely accounted for 24.6 % of nucleation particle formation, and the maximal values of net increase rate and formation rate were in the same heating day (period after 15 November of campaign И was considered in heating period). Heating might provide persistent precursors for NPF, and its acceleration was particularly evident in December. Another notable period was from 10 October to 18 October 2014, during which it had frequent NPF events and most of formation rates were larger than 75th percentile (20.61 cm^{-3} s^{-1}). It could be associated with specific atmospheric conditions because of sudden temperature drop. Mountain observations on Mt. Huang (869 ASL) and Mt. Daban (3295 ASL) in China didn't report formation rates, while the average formation rate on Mt. Tai was significantly larger than 2.94 cm^{-3} s^{-1} at the waist of Mt. Tai Mo Shan (640 ASL). Moreover it found formation rate on Mt. Tai was also obviously larger than other air mass style observations shown in Table 3, including preponderant marine and urban environments (Liu et al., 2014; Zhu et

Atmos. Chem. Phys. Discuss., doi:10.5194/acp-2016-806, 2016
Manuscript under review for journal Atmos. Chem. Phys.
Published: 24 October 2016

al., 2014; Wang et al., 2015; Xiao et al., 2015). Reasons for our large value were possibly not only related to geographically wide mountaintop location, but also sampling season impacts and size range difference for calculating formation rate.

Growth rates on Mt. Tai ranged from 0.58 to 7.76 nm h^{-1}, and their median, 25th percentile and 75th percentile were separately 1.55, 1.15 and 2.51 nm h^{-1}. Growth rates on Mt. Tai could be comparable with 3.86 nm h^{-1} at Mt. Tai Mo Shan, 3.58 nm h^{-1} on Mt. Huang and 2.0 nm h^{-1} on Mt. Daban (Du et al., 2015; Guo et al., 2012; Hao et al., 2015). In Table 3, either less polluted rural/suburban sites such as Backgarden or fickle urban sites such as Shanghai trended to reveal larger growth rate than mountain observations, especially for higher-elevation sites on Mt. Daban and Mt. Tai (Yue et al., 2013; Liu et al., 2008; Gao et al., 2011; Qi et al., 2015; Xiao et al., 2015). It inferred that clean mountain environments with less anthropogenic impacts possibly weakened newly formed particle growth.

Condensation sinks were in the range of 0.40×10^{-2}-6.32×10^{-2} s^{-1} for valid data during this study, and the values were comparable with 0.6×10^{-2}-8.4×10^{-2} s^{-1} in Beijing, 0.9×10^{-2}-3.9×10^{-2} s^{-1} in Nanjing, and 1.0×10^{-2}-6.2×10^{-2} s^{-1} in Hong Kong (Zhang et al., 2011; Gao et al., 2012; Guo et al., 2012; An et al., 2015; Herrmann et al., 2014). Mean sulfur dioxide concentrations during nucleation processes were 0.18-17.54 ppb. As shown in Fig. 1, sulfur dioxide on NPF days tended to be slightly larger value than that on non-NPF days, but this increase was not significant. Although gaseous sulfuric acid formed through sulfur dioxide photochemical reactions was involved in NPF, neither high sulfur dioxide being strong NPF nor low value limiting NPF burst. Song et al. (2010) found that sulfur dioxide increased or decreased before NPF, and weak sensitivity between NPF events and sulfur dioxide suggested a coupling of sulfuric acid and pre-existing particles. Large condensation sink implied a high concentration of pre-existing particles which act as the sink for condensing vapors and newly formed particles. Wang et al. (2011) reported that condensation sink on NPF days was typically lower than that on non-NPF days in Beijing cases, while it didn't exhibit significant distinction in our work and most condensation sink values were smaller than 0.02 s^{-1} on both NPF and non-NPF days. Moreover all the condensation sinks larger than 0.02 s^{-1} on NPF days in Fig. 1 occurred during the late period of NPF events (about 9:00-11:00 LT), indicating low pre-existing particles existing in Mt. Tai environment and weak limiting of pre-existing particles for most NPF occurrence.

3.2 Sulfuric acid contribution analysis

Gas-phase sulfuric acid has been identified as a vital precursor during the whole NPF processes, and photochemical oxidation from sulfur dioxide is a significant source in the atmosphere. Direct measurement of gaseous sulfuric acid was not available in this work, but it could roughly estimate sulfuric acid concentration using sulfur dioxide and solar radiation data to evaluate the role of gaseous sulfuric acid for NPF.

Sulfuric acid proxies at the beginning of nucleation particles enhancing were in the range of 0.56×10^{6}-25.40×10^{6} cm^{-3}. McMurry et al. (2005) reported that NPF events could be detected when the sulfuric acid concentration got above 5×10^{6} cm^{-3}, while half of our estimations in Table 1 were smaller than this critical value. Great uncertainty of solar radiation in this study

Atmos. Chem. Phys. Discuss., doi:10.5194/acp-2016-806, 2016
Manuscript under review for journal Atmos. Chem. Phys.
Published: 24 October 2016

Atmospheric Chemistry and Physics Discussions

might account for the dominant error for underestimating sulfuric acid values in the atmosphere.

Sulfuric acid condensation could contribute to the newly formed particle growth, and growth rate fraction for sulfuric acid by Eq. (6) was estimated in Table 1 and Table 2. The growth rates determined by sulfuric acid proxies varied from 0.03 to 1.19 nm h^{-1}, and mean ratio of GR-C to GR was 16.20 %. Compared with the estimations of 8-13 % at Idaho Hill, Colorad (Weber et al., 1997) and 4-31 % in Hyytiälä, Finland (Boy et al., 2003; Boy et al., 2005), growth rate fractions for sulfuric acid on Mt. Tai were in a broad range (0.61-72.66 %). Because of errors existing in sulfuric acid estimation, the exceptionally high values seemed not to be credible. However, the 25th percentile (5.92 %) and 75th percentile (22.63 %) could be comparable with above reported results, and it was plausible that sulfuric acid condensation also made significant contribution on particle further growth on Mt. Tai.

As the vital nucleation precursor, sulfuric acid was thus associated with the freshly nucleation particles. It found that the sulfuric acid proxies on most of NPF days showed evident correlation with the total particle number concentration of 3-6 nm ($N_{3\text{-}6\ nm}$), and this correlation was consistent with reported researches (Kulmala et al., 2006; Wang et al., 2011). As an example in Fig. 2, the curves of $N_{3\text{-}6\ nm}$ and $[H_2SO_4]^{1.75}$ reflected a moderate correlation (R^2 =0.622) on 15 October 2014 and time delay between them could almost be neglected. In Wang et al. (2011) studies, it reported the fore-formed nucleated particles and rapid growth might account for such no time delay. Most calculated power exponents of $N_{3\text{-}6\ nm}$ and $[H_2SO_4]$ approximated 1 on Mt. Tai, but these values required further investigation because of non-confidence for sulfuric acid estimation.

3.3 Gas species, meteorological conditions and air mass backward trajectories during NPF

Figure 3 picked 40 days continuous data from 31 October to 9 December 2014 for intensive NPF occurrence to visually show the influence of gas species and meteorological factors on NPF events, and shaded areas represented the NPF days.

Mean concentration of sulfur dioxide on all NPF days was 3.5 ppb, while the value was only 2.4 ppb on non-NPF days. Sulfur dioxide almost exhibited 46 % preponderance on NPF days, and this result was in accordance with the former discussion in Sect. 3.1. Although it didn't make the immediate relationship between sulfur dioxide and NPF, higher sulfur dioxide could improve the possibility of rich precursors for NPF. For instance in Fig. 3, sulfur dioxide appeared to be exceptionally high values because of sudden drop in temperature from 30 November to 8 December 2014, and during this period NPF events had frequent occurrence. It could be interpreted that drop in temperature enhanced heating activities and sources for sulfur dioxide would increase in accompany.

Average ozone values on all NPF days and non-NPF days were separately 31.5 ppb and 35.0 ppb, and the difference was minimal compared with sulfur dioxide. Existent of ozone could quantify the oxidation capacity and photochemical activities in the atmosphere, directly reacting with related species such as VOCs and indirectly affecting sulfuric acid formation via hydroxyl radical production (Berndt et al., 2010; Gómez Martín et al., 2013; Sorribas et al., 2015). Based on daily analysis

Atmos. Chem. Phys. Discuss., doi:10.5194/acp-2016-806, 2016
Manuscript under review for journal Atmos. Chem. Phys.
Published: 24 October 2016

on Mt. Tai, it found ozone concentration revealed slight drop during nucleation process on many NPF days and ozone consumption reactions might take place.

Song et al. (2010) reported that favorable meteorological conditions made for NPF when precursors were insufficient in the atmosphere, and our statistical results showed that NPF preferred to occur on clear or partial cloudy daytime. Daily averages of temperature for all NPF days varied from -11.8 to 22.1 ℃, and the values of relative humidity were in the range of 22-95 %. Day-to-day analysis revealed that temperature and relative humidity always had cyclic variation, and NPF events preferably occurred on high temperature and low relative humidity conditions. High temperature and low humidity could promote vertical transportation and photochemical reactions in the atmosphere (O'Dowd, 2002; An et al., 2015).

NPF days had a wide range of wind speed (0.2-7.8 m s^{-1}), and wind speed influence on NPF might be minimal. Compared with non-NPF days, the wind direction on NPF days had more narrow range and NPF events typically took place in west-southwest and east-southeast directions (Fig. 4a). It meant that the regional point sources such as some heavy industries from above two directions might increase the probability of NPF occurrence in a certain extent if there was upward or vertical transportation. Particle number concentrations depending on wind direction in each mode were not obvious, and none of directions always showed significantly higher or smaller particle concentrations and it had clear difference with reports in Nanjing (Herrmann et al., 2014). It could suggest that few direct particle pollution sources existed around observation site and nucleation might be the primary source for particles on Mt. Tai.

Air mass backward trajectories at 1535 m ASL were analyzed in Fig. 5, and they were simulated using HYSPLIT model developed by the National Oceanic and Atmospheric Administration (NOAA) Air Resources Laboratory. Figure 5a illustrated the air mass backward trajectories of all NPF days for 72 h at 6:00 LT, and the magenta pathways were haze days with NPF occurrence, namely NPF haze days, for latter discussion in Sect. 3.6.

The majority of transport pathways on Mt. Tai during NPF days came from northwest, and this direction was mainly influenced by Siberia monsoon. The northwest air masses largely originated from Siberia and passed over Mongolia, Inner Mongolia, Shanxi Province, Hebei Province, Beijing et al. at fast or moderate speed. Compared with air masses coming from cleaner western parts of China, air masses going through Beijing et al. polluted areas had more complicated components and enhanced NPF events. Besides, local continental and maritime backward trajectories also existed during our observation. Local continental air masses were largely from surroundings such as Jinan, Nanjing, Zhengzhou, while maritime air masses passed though marginal areas of Bohai Sea (B-S) and Yellow Sea (Y-S). In addition, local pathways trended to be upward air masses coming from lower layer of observation site, while long-distance continental air masses were more likely to transport from upper atmospheric layer. Hence NPF events with local continental backward trajectories were more vulnerable to local point sources.

3.4 $PM_{2.5}$ variation during NPF days

Atmos. Chem. Phys. Discuss., doi:10.5194/acp-2016-806, 2016
Manuscript under review for journal Atmos. Chem. Phys.
Published: 24 October 2016

Atmospheric Chemistry and Physics Discussions

Daily average $PM_{2.5}$ on all NPF days was 31 μg m^{-3}, while the value on non-NPF days was 40 μg m^{-3}. Pre-existing particles in the atmosphere were against the newly formed particles and low $PM_{2.5}$ condition seemed to be favorable for nucleation. In Fig. 6, it also picked the data from 31 October to 9 December 2014 to further investigate the relationship between $PM_{2.5}$ and NPF events.

Influenced by the daytime activities, $PM_{2.5}$ showed higher values in the most daytime and this phenomenon was more evident on NPF days. Statistics found that $PM_{2.5}$ would obviously trend to increase in two hours after more than 90 % of NPF occurrence. Most values of $PM_{2.5}$ at the beginning of each increase on above NPF days were less than 15 μg m^{-3}, and peak $PM_{2.5}$ varied a lot under different conditions. In campaign I peak $PM_{2.5}$ showed the maximum (mostly near 140 μg m^{-3}), while in late campaign И it was the minimum (generally less than 80 μg m^{-3}). The higher atmospheric humidity in campaign I might enhance the sticking possibility of particles for molecules, and hygroscopic growth of growing particles would be a significant factor for above difference. In addition, sometimes $PM_{2.5}$ almost remained in constant and low level during NPF period, which always occurred in enhanced atmospheric dilution or intense meteorological change condition.

In campaign И, more than three-quarters of growth rates were less than 2.0 nm h^{-1}, and daily average $PM_{2.5}$ on these NPF days was 26 μg m^{-3} while the others in campaign И was 48 μg m^{-3}. The similar difference could also be seen in Fig. 6, and the large growth rates seemed to be in higher $PM_{2.5}$ days. Newly formed particles could condense on pre-existing particles, thus high $PM_{2.5}$ condition suppressed NPF occurrence. As independent processes of nucleation and growth, it might be plausible that this suppression of high $PM_{2.5}$ was mainly against nucleation rather than growth. It speculated that hygroscopic growth would not be significant in campaign И, but particles recombination in close sizes could contribute to the growth after nucleation and higher $PM_{2.5}$ within limiting values possibly increased this possibility. However, this speculation wasn't reported in previous researches and its accuracy required further investigation in other environments.

3.5 NPF events on clean and polluted conditions

According to the Chinese Meteorological Administration (CMA), a day could be roughly identified as polluted day if its daily average $PM_{2.5}$ is larger than 75 μg m^{-3}. Closer particle behaviors on clean day (29 September 2014) and polluted day (8 November 2014) were typically presented in Fig. 7, and different measuring ranges of NAIS and WPS provided a complete size distribution in whole nucleation and growth processes.

Normally background value of total nucleation particles approximated several hundreds of particles per cubic centimeter, while the concentration would rapidly increase 100 to 1,000 times when an NPF event occurred. As shown in Fig. 7 (a-c), new nucleation mode particles obviously appeared at about 8:00 LT on 29 September 2014, and its concentration rose from 200 to 2.5×10^{5} cm^{-3}. Particles grew several hours, and the sizes reached their maximum of ~200 nm at about 16:00 LT. During the first growth period, the geometric median diameter (GMD) of nucleation particles approximated to be linear growth which varied from 5.3 to 13.6 nm and fitted the growth rate as 1.13 nm h^{-1} with least square method. Evolution of

Atmos. Chem. Phys. Discuss., doi:10.5194/acp-2016-806, 2016
Manuscript under review for journal Atmos. Chem. Phys.
Published: 24 October 2016

particle number concentration in size of 2-3 nm, 3-20 nm (nucleation mode), 20-100 nm (Aitken mode) and 100-200 nm (accumulation mode) in Fig. 7d revealed that fine particles on Mt Tai largely existed as Aitken mode before NPF occurrence on clean condition. Particles formed though NPF accounted for the majority of nucleation mode at first, and then they mainly contributed to Aitken mode eventually and only the minority could grow above 100 nm. After 19:00 LT, particle number concentrations in each size sharply decreased because of atmospheric scavenging and they almost returned to background values. By contrast, particles in Aitken and accumulation modes made up the major percentage of volume concentration whether NPF event occurred or not. Evolution of volume concentration stack column was in accordance with the $PM_{2.5}$ curve in Fig. 7e, and they reached the maximums at about 15:00 LT. Gap between them would particularly increase during NPF period, indicating particles growing over 200 nm made significant contribution to $PM_{2.5}$. If particles in the atmosphere were assumed as the spheres, it would find that particle density on clean day approximated less than 1 g cm^{-3} on Mt. Tai based on volume concentration and $PM_{2.5}$ values.

In contrast, background total nucleation particles on 8 November 2014 were about 1200 cm^{-3} and increased to the maximum of 7.0×10^4 cm^{-3} at about 10:00 LT. The GMD varied from 4.3 to 11.1 nm with the growth rate of 2.95 nm h^{-1}. On polluted condition, particles in Aiken and accumulation modes always existed with high values in the atmosphere, and NPF event showed weaker and lasted shorter because of possible impact of pre-existing particles. Newly formed particles also largely contributed to Aiken mode finally similar to the clean day, and $PM_{2.5}$ variation was consistent with volume concentration as well. However, NPF had small impact on total volume concentration on polluted day, which might be related to large background fine particles. In addition, the obvious increase in accumulation mode after 12:00 LT in Fig. 7j was mainly because of transfer air masses.

3.6 NPF events on haze and non-haze conditions

Combination visibility with relative humidity, it found that most NPF events occurred on clear days and there statistically existed in four NPF events on haze condition in our study. Although only four NPF events occurred on haze condition, a number of haze episodes were observed after hours of NPF on Mt. Tai and it might imply NPF was likely to be one of induction factors for haze formation. Daily average $PM_{2.5}$ on all haze days was 64 μg m^{-3} and the value on four NPF haze days was 63 μg m^{-3}, between which it showed no obvious difference. NPF events could still occur under such high $PM_{2.5}$ condition, and it seemed that some specific substances or mechanisms might exist.

Figure 5 (b-e) presented the air mass backward trajectories for 24 h at 4:00, 6:00, 8:00 and 10:00 LT on four NPF haze days, and the magentas in Fig. 5a were their backward pathways for 72 h at 6:00 LT. Air masses on 26 July 2014 passed through Bohai Sea for hours before arriving at observation site, which probably brought motivating substances promoting NPF. On 17 October and 18 October 2014, the trajectories of both days for 72 h had sudden change at the adjacent locations where might be local point sources for some precursors (see Fig. 5a, 5c, 5d). On 11 November 2014, it revealed

Atmos. Chem. Phys. Discuss., doi:10.5194/acp-2016-806, 2016
Manuscript under review for journal Atmos. Chem. Phys.
Published: 24 October 2016

exceptionally high ammonia with average value of 72.3 ppb, and ammonia seemed to contribute to the nucleation on this NPF haze day.

Three typical cases on NPF haze day (18 October 2014), NPF non-haze day (17 November 2014) and non-NPF haze day (20 November 2014) were specially discussed in Fig. 8. It illustrated that on both haze days particle number concentrations in 2 nm, 3 nm, 20 nm and 40 nm didn't show distinct difference if there was not any nucleation burst or sudden air mass transportation. On NPF haze day peak values in 2 nm, 3 nm and 20 nm were in close level, which might be related to the persistent specific precursors in the atmosphere. In contrast, on NPF non-haze day peak value in 3 nm was much larger than that in 2 nm, while concentrations in 20 nm and 40 nm dropped a lot compared with 3 nm. Reason for the former was possibly clusters recombination, and the latter decrease might be on account of energy threshold (i.e., nucleation barrier) and atmospheric scavenging. In addition, from the curves in Fig. 8 it found that particles burst in each size on NPF haze day almost had no time lag (about 12:45 LT), while variations on NPF non-haze day existed in distinct time lag and it could observe the growth process visually. Moreover, the increase of particle number concentration in each size on NPF haze day was rapider and shorter-time compared with NPF non-haze day.

4. Conclusions

Field observations of NPF at the mountain-tops are scarce in China and its related researches could significantly contribute to atmospheric aerosol pollution control. A comprehensive investigation of NPF was conducted at the summit of Mt. Tai (1530 m ASL) from 25 July to 24 October 2014 (I), 21 September to 9 December 2014 (И) and 16 June to 7 August 2015 (Ш), using two types of size distribution instruments (NAIS and WPS) and including two gaseous pollutants, multiple meteorological parameters and $PM_{2.5}$. During the 164 days of observation, 66 NPF events were identified overall giving an occurrence frequency of 40 %. Formation rates, growth rates and condensation sinks were in the range of 1.10-57.43 cm^{-3} s^{-1}, 0.58-7.76 nm h^{-1} and 0.40×10^{-2}-6.32×10^{-2} s^{-1} respectively. In comparison with other studies in China, it found that Mt. Tai had the larger formation rate and its growth rate trended to be smaller. Condensation sinks on NPF days and non-NPF days showed no significant difference, and low pre-existing particles existed and weak limitation of pre-existing particles for NPF in Mt. Tai environment.

Sulfuric acid proxies estimated by sulfur dioxide and solar radiation varied from 0.56×10^{6} to 25.40×10^{6} cm^{-3} when the nucleation particles enhanced, and growth rate fractions for sulfuric acid averaged 16.20 %. Without consideration errors of sulfuric acid proxies, the $N_{3\text{-}6\ nm}$ and sulfuric acid showed an evident correlation with the power exponents of about 1 for most NPF days. The mean sulfur dioxide concentration on NPF days was 46 % larger than that on non-NPF days, and sulfur dioxide with higher value could indirectly enhance NPF occurrence. High temperature and low relative humidity were favorable for NPF, and NPF events were more common when the wind was from the west-southwest and east-southeast

directions. There were mainly three types of air mass backward trajectories for 72 h on all NPF days, and the majority came from the northwest.

Daily average $PM_{2.5}$ on all NPF days was lower than that on non-NPF days, suggesting that lower $PM_{2.5}$ values encouraged nucleation. $PM_{2.5}$ could increase after more than 90 % of NPF occurrence, and hygroscopic growth might make significant impact on the peak of $PM_{2.5}$. In campaign И, NPF days with limited higher $PM_{2.5}$ trended to be large growth rates, and this might be accounted for particles recombination in close sizes. NPF events on clean/polluted and haze/non-haze conditions showed characteristic behaviors, and typical conditions had effective influence on NPF. Only four NPF events occurred on haze episodes on Mt. Tai during our observation, and it was clear that specific mechanisms or substances were responsible for the NPF under haze condition with such high $PM_{2.5}$.

Acknowledgements. This work was supported by National Natural Science Foundation of China (No. 41375126), Mount Tai Scholar Grand (ts20120552), Cyrus Tang Foundation (No.CTF-FD2014001), Ministry of Science and Technology of China (SQ2016ZY01002231, 2014BAC22B01), and Marie Skłodowska-Curie Actions (H2020-MSCA-RISE-2015-690958).

References

Allan, J. D., Williams, P. I., Najera, J., Whitehead, J. D., Flynn, M. J., Taylor, J. W., Liu, D., Darbyshire, E., Carpenter, L. J., Chance, R., Andrews, S. J., Hackenberg, S. C., and McFiggans, G.: Iodine observed in new particle formation events in the Arctic atmosphere during ACCACIA, Atmos. Chem. Phys., 15, 5599-5609, doi:10.5194/acp-15-5599-2015, 2015.

An, J., Wang, H., Shen, L., Zhu, B., Zou, J., Gao, J., and Kang, H.: Characteristics of new particle formation events in Nanjing, China: Effect of water-soluble ions, Atmos. Environ., 108, 32-40, doi:10.1016/j.atmosenv.2015.01.038, 2015.

Berndt, T., Stratmann, F., Sipilä, M., Vanhanen, J., Petäjä, T., Mikkilä, J., Grüner, A., Spindler, G., Lee Mauldin Iii, R., Curtius, J., Kulmala, M., and Heintzenberg, J.: Laboratory study on new particle formation from the reaction OH + SO_2 : influence of experimental conditions, H_2O vapour, NH_3 and the amine tert-butylamine on the overall process, Atmos. Chem. Phys., 10, 7101-7116, doi:10.5194/acp-10-7101-2010, 2010.

Boy, M., Rannik, Ü., Lehtinen, K. E. J., Tarvainen, V., Hakola, H., and Kulmala, M.: Nucleation events in the continental boundary layer: Long-term statistical analyses of aerosol relevant characteristics, J. Geophys. Res., 108, 4667, doi:10.1029/2003jd003838, 2003.

Boy, M., Kulmala, M., Ruuskanen, T. M., Pihlatie, M., Reissell, A., Aalto, P. P., Keronen, P., Dal Maso, M., Hellen, H., Hakola, H., Jansson, R., Hanke, M., and Arnold, F.: Sulphuric acid closure and contribution to nucleation mode particle growth, Atmos. Chem. Phys., 5, 863-878, doi:10.5194/acp-5-863-2005, 2005.

Dal Maso, M., Kulmala, M., Lehtinen, K. E. J., Mäkelä, J. M., Aalto, P., and O'Dowd, D.: Condensation and coagulation

sinks and formation of nucleation mode particles in coastal and boreal forest boundary layers, J. Geophys. Res., 107, 8097, doi:10.1029/2001JD001053, 2002.

Dal Maso, M., Kulmala, M., Riipinen, I., Wagner, R., Hussein, T., Aalto, P. P., and Lehtinen, K. E. J.: Formation and growth of fresh atmospheric aerosols : Eight Years of Aerosol Size Distribution Data from SMEAR II, Hyytiälä, Finland, Boreal Environ. Res., 10, 323-336, 2005.

Du, W., Sun, Y. L., Xu, Y. S., Jiang, Q., Wang, Q. Q., Yang, W., Wang, F., Bai, Z. P., Zhao, X. D., and Yang, Y. C.: Chemical characterization of submicron aerosol and particle growth events at a national background site (3295 m a.s.l.) in the Tibetan Plateau, Atmos. Chem. Phys. Discussions, 15, 13515-13550, doi:10.5194/acpd-15-13515-2015, 2015.

Fuchs, N. A.: The mechanics of aerosols, 1964.

Gómez Martín, J. C., Gálvez, O., Baeza-Romero, M. T., Ingham, T., Plane, J. M., and Blitz, M. A.: On the mechanism of iodine oxide particle formation, Phys. Chem. Chem. Phys., 15, 15612-15622, doi:10.1039/c3cp51217g, 2013.

Gao, J., Wang, T., Zhou, X., Wu, W., and Wang, W.: Measurement of aerosol number size distributions in the Yangtze River delta in China: Formation and growth of particles under polluted conditions, Atmos. Environ., 43, 829-836, doi:10.1016/j.atmosenv.2008.10.046, 2009.

Gao, J., Chai, F., Wang, T., and Wang, W.: Particle number size distribution and new particle formation (NPF) in Lanzhou, Western China, Particuology, 9, 611-618, doi:10.1016/j.partic.2011.06.008, 2011.

Gao, J., Chai, F., Wang, T., Wang, S., and Wang, W.: Particle number size distribution and new particle formation: New characteristics during the special pollution control period in Beijing, J. Environ. Sci., 24, 14-21, doi:10.1016/s1001-0742(11)60725-0, 2012.

Gong, Y., Hu, M., Cheng, Y., Su, H., Yue, D., Liu, F., Wiedensohler, A., Wang, Z., Kalesse, H., and Liu, S.: Competition of coagulation sink and source rate: New particle formation in the Pearl River Delta of China, Atmos. Environ., 44, 3278-3285, doi:10.1016/j.atmosenv.2010.05.049, 2010.

Guo, H., Wang, D. W., Cheung, K., Ling, Z. H., Chan, C. K., and Yao, X. H.: Observation of aerosol size distribution and new particle formation at a mountain site in subtropical Hong Kong, Atmos. Chem. Phys., 12, 9923-9939, doi:10.5194/acp-12-9923-2012, 2012.

Hallar, A. G., Lowenthal, D. H., Chirokova, G., Borys, R. D., and Wiedinmyer, C.: Persistent daily new particle formation at a mountain-top location, Atmos. Environ., 45, 4111-4115, doi:10.1016/j.atmosenv.2011.04.044, 2011.

Han, S.: Effect of Aerosols on Visibility and Radiation in Spring 2009 in Tianjin, China, Aerosol Air Qual. Res., 12, 211-217, doi:10.4209/aaqr.2011.05.0073, 2012.

Hao, J., Yin, Y., Li, X., Yuan, L., and Xiao, H.: Observations of Nucleation Mode Particles Formation and Growth on Mount Huang, China, Procedia Engineering, 102, 1167-1176, doi:10.1016/j.proeng.2015.01.242, 2015.

Herrmann, E., Ding, A. J., Kerminen, V. M., Petäjä, T., Yang, X. Q., Sun, J. N., Qi, X. M., Manninen, H., Hakala, J.,

Nieminen, T., Aalto, P. P., Kulmala, M., and Fu, C. B.: Aerosols and nucleation in eastern China: first insights from the new SORPES-NJU station, Atmos. Chem. Phys., 14, 2169-2183, doi:10.5194/acp-14-2169-2014, 2014.

Kanawade, V. P., Shika, S., Pöhlker, C., Rose, D., Suman, M. N. S., Gadhavi, H., Kumar, A., Nagendra, S. M. S., Ravikrishna, R., Yu, H., Sahu, L. K., Jayaraman, A., Andreae, M. O., Pöschl, U., and Gunthe, S. S.: Infrequent occurrence of new particle formation at a semi-rural location, Gadanki, in tropical Southern India, Atmos. Environ., 94, 264-273, doi:10.1016/j.atmosenv.2014.05.046, 2014.

Kuang, C., Riipinen, I., Sihto, S. L., Kulmala, M., McCormick, A. V., and McMurry, P. H.: An improved criterion for new particle formation in diverse atmospheric environments, Atmos. Chem. Phys., 10, 8469-8480, doi:10.5194/acp-10-8469-2010, 2010.

Kulmala, M., Dal Maso, M., Mäkelä, M., Pirjola, L., Väkevä, M., Aalto, P., Miikkulainen, P., and Hämeri, K.: On the formation, growth and composition of nucleation mode particles, Tellus B, 53, 479-490, doi:10.1034/j.1600-0889.2001.d01-33.x, 2001.

Kulmala, M.: How particles nucleate and grow, Science, 302, 1000-1001, doi:10.1126/science.1090848, 2003.

Kulmala, M., Vehkamäki, H., Petäjä, T., Dal Maso, M., Lauri, A., Kerminen, V. M., Birmili, W., and McMurry, P. H.: Formation and growth rates of ultrafine atmospheric particles: a review of observations, J. Aerosol Sci., 35, 143-176, doi:10.1016/j.jaerosci.2003.10.003, 2004.

Kulmala, M., Lehtinen, K. E. J., and Laaksonen, A.: Cluster activation theory as an explanation of the linear dependence between formation rate of 3 nm particles and sulphuric acid concentration, Atmos. Chem. Phys., 6, 787-793, doi:10.5194/acp-6-787-2006, 2006.

Kulmala, M., Petäjä, T., Nieminen, T., Sipila, M., Manninen, H. E., Lehtipalo, K., Dal Maso, M., Aalto, P. P., Junninen, H., Paasonen, P., Riipinen, I., Lehtinen, K. E., Laaksonen, A., and Kerminen, V. M.: Measurement of the nucleation of atmospheric aerosol particles, Nat. Protoc., 7, 1651-1667, doi:10.1038/nprot.2012.091, 2012.

Li, W. J., Zhang, D. Z., Shao, L. Y., Zhou, S. Z., and Wang, W. X.: Individual particle analysis of aerosols collected under haze and non-haze conditions at a high-elevation mountain site in the North China plain, Atmos. Chem. Phys., 11, 11733-11744, doi:10.5194/acp-11-11733-2011, 2011.

Liu, S., Hu, M., Wu, Z., Wehner, B., Wiedensohler, A., and Cheng, Y.: Aerosol number size distribution and new particle formation at a rural/coastal site in Pearl River Delta (PRD) of China, Atmos. Environ., 42, 6275-6283, doi:10.1016/j.atmosenv.2008.01.063, 2008.

Liu, X. H., Zhu, Y. J., Zheng, M., Gao, H. W., and Yao, X. H.: Production and growth of new particles during two cruise campaigns in the marginal seas of China, Atmos. Chem. Phys., 14, 7941-7951, doi:10.5194/acp-14-7941-2014, 2014.

Manninen, H. E., Nieminen, T., Asmi, E., Gagné, S., Häkkinen, S., Lehtipalo, K., Aalto, P., Vana, M., Mirme, A., Mirme, S., Hõrrak, U., Plass-Dülmer, C., Stange, G., Kiss, G., Hoffer, A., Törő, N., Moerman, M., Henzing, B., de Leeuw, G.,

Brinkenberg, M., Kouvarakis, G. N., Bougiatioti, A., Mihalopoulos, N., O'Dowd, C., Ceburnis, D., Arneth, A., Svenningsson, B., Swietlicki, E., Tarozzi, L., Decesari, S., Facchini, M. C., Birmili, W., Sonntag, A., Wiedensohler, A., Boulon, J., Sellegri, K., Laj, P., Gysel, M., Bukowiecki, N., Weingartner, E., Wehrle, G., Laaksonen, A., Hamed, A., Joutsensaari, J., Petäjä, T., Kerminen, V. M., and Kulmala, M.: EUCAARI ion spectrometer measurements at 12 European sites-analysis of new particle formation events, Atmos. Chem. Phys., 10, 7907-7927, doi:10.5194/acp-10-7907-2010, 2010.

McMurry, P. H., Fink, M., Sakurai, H., Stolzenburg, M. R., Mauldin, R. L., Smith, J., Eisele, F., Moore, K., Sjostedt, S., Tanner, D., Huey, L. G., Nowak, J. B., Edgerton, E., and Voisin, D.: A criterion for new particle formation in the sulfur-rich Atlanta atmosphere, J. Geophys. Res., 110, 2935-2948, doi:10.1029/2005jd005901, 2005.

Meng, H., Zhu, Y., Evans, G. J., Jeong, C. H., and Yao, X.: Roles of SO_2 oxidation in new particle formation events, J. Environ. Sci. (China), 30, 90-101, doi:10.1016/j.jes.2014.12.002, 2015.

Mikkonen, S., Romakkaniemi, S., Smith, J. N., Korhonen, H., Petäjä, T., Plass-Duelmer, C., Boy, M., McMurry, P. H., Lehtinen, K. E. J., Joutsensaari, J., Hamed, A., Mauldin Iii, R. L., Birmili, W., Spindler, G., Arnold, F., Kulmala, M., and Laaksonen, A.: A statistical proxy for sulphuric acid concentration, Atmos. Chem. Phys. Discussions, 11, 20141-20179, doi:10.5194/acpd-11-20141-2011, 2011.

O'Dowd, C. D.: A dedicated study of New Particle Formation and Fate in the Coastal Environment (PARFORCE): Overview of objectives and achievements, J. Geophys. Res., 107, 8108, doi:10.1029/2001jd000555, 2002.

Qi, X. M., Ding, A. J., Nie, W., Petäjä, T., Kerminen, V. M., Herrmann, E., Xie, Y. N., Zheng, L. F., Manninen, H., Aalto, P., Sun, J. N., Xu, Z. N., Chi, X. G., Huang, X., Boy, M., Virkkula, A., Yang, X. Q., Fu, C. B., and Kulmala, M.: Aerosol size distribution and new particle formation in western Yangtze River Delta of China: two-year measurement at the SORPES station, Atmos. Chem. Phys., 15, 12491-12537, doi:10.5194/acpd-15-12491-2015, 2015.

Qi, Z., Stanier, C. O., Canagaratna, M. R., Jayne, J. T., and Worsnop, D. R.: Insights into the chemistry of new particle formation and growth events in Pittsburgh based on aerosol mass pectrometry, Environ. Sci. Technol., 38, 4797-4809, doi:10.1021/es035417u, 2004.

Saunders, R. W., Kumar, R., Martin, J. C. G., Mahajan, A. S., Murray, B. J., and Plane, J. M. C.: Studies of the Formation and Growth of Aerosol from Molecular Iodine Precursor, Z. Phys. chem., 224, 1095-1117, doi:10.1524/zpch.2010.6143, 2010.

Setyan, A., Song, C., Merkel, M., Knighton, W. B., Onasch, T. B., Canagaratna, M. R., Worsnop, D. R., Wiedensohler, A., Shilling, J. E., and Zhang, Q.: Chemistry of new particle growth in mixed urban and biogenic emissions-insights from CARES, Atmos. Chem. Phys., 14, 6477-6494, doi:10.5194/acp-14-6477-2014, 2014.

Smith, J. N., Dunn, M. J., VanReken, T. M., Iida, K., Stolzenburg, M. R., McMurry, P. H., and Huey, L. G.: Chemical composition of atmospheric nanoparticles formed from nucleation in Tecamac, Mexico: Evidence for an important role for

organic species in nanoparticle growth, Geophys. Res. Lett., 35, doi:10.1029/2007gl032523, 2008.

Song, M., Lee, M., Kim, J. H., Yum, S. S., Lee, G., and Kim, K.-R.: New particle formation and growth in relation to vertical mixing and chemical species during ABC-EAREX2005, Atmos. Res., 97, 359-370, doi:10.1016/j.atmosres.2010.04.013, 2010.

Sorribas, M., Adame, J. A., Olmo, F. J., Vilaplana, J. M., Gil-Ojeda, M., and Alados-Arboledas, L.: A long-term study of new particle formation in a coastal environment: meteorology, gas phase and solar radiation implications, Sci. Total Environ., 511, 723-737, doi:10.1016/j.scitotenv.2014.12.011, 2015.

Spracklen, D. V., Carslaw, K. S., Kulmala, M., Kerminen, V.-M., Sihto, S.-L., Riipinen, I., Merikanto, J., Mann, G. W., Chipperfield, M. P., Wiedensohler, A., Birmili, W., and Lihavainen, H.: Contribution of particle formation to global cloud condensation nuclei concentrations, Geophys. Res. Lett., 35, doi:10.1029/2007gl033038, 2008.

Wang, D., Guo, H., Cheung, K., and Gan, F.: Observation of nucleation mode particle burst and new particle formation events at an urban site in Hong Kong, Atmos. Environ., 99, 196-205, doi:10.1016/j.atmosenv.2014.09.074, 2014a.

Wang, H., Zhu, B., Shen, L., An, J., Yin, Y., and Kang, H.: Number size distribution of aerosols at Mt. Huang and Nanjing in the Yangtze River Delta, China: Effects of air masses and characteristics of new particle formation, Atmos. Res., 150, 42-56, doi:10.1016/j.atmosres.2014.07.020, 2014b.

Wang, Z. B., Hu, M., Yue, D. L., Zheng, J., Zhang, R. Y., Wiedensohler, A., Wu, Z. J., Nieminen, T., and Boy, M.: Evaluation on the role of sulfuric acid in the mechanisms of new particle formation for Beijing case, Atmos. Chem. Phys., 11, 12663-12671, doi:10.5194/acp-11-12663-2011, 2011.

Wang, Z. B., Hu, M., Pei, X. Y., Zhang, R. Y., Paasonen, P., Zheng, J., Yue, D. L., Wu, Z. J., Boy, M., and Wiedensohler, A.: Connection of organics to atmospheric new particle formation and growth at an urban site of Beijing, Atmos. Environ., 103, 7-17, doi:10.1016/j.atmosenv.2014.11.069, 2015.

Weber, R. J., Marti, J. J., McMurry, P. H., Eisele, F. L., Tanner, D. J., and Jefferson, A.: Measurements of new particle formation and ultrafine particle growth rates at a clean continental site, J. Geophys. Res., 102, 4375, doi:10.1029/96jd03656, 1997.

Wehner, B., Wiedensohler, A., Tuch, T. M., Wu, Z. J., Hu, M., Slanina, J., and Kiang, C. S.: Variability of the aerosol number size distribution in Beijing, China: New particle formation, dust storms, and high continental background, Geophys. Res. Lett., 31, doi:10.1029/2004gl021596, 2004.

Xiao, S., Wang, M. Y., Yao, L., Kulmala, M., Zhou, B., Yang, X., Chen, J. M., Wang, D. F., Fu, Q. Y., Worsnop, D. R., and Wang, L.: Strong atmospheric new particle formation in winter in urban Shanghai, China, Atmos. Chem. Phys., 15, 1769-1781, doi:10.5194/acp-15-1769-2015, 2015.

Yue, D. L., Hu, M., Wang, Z. B., Wen, M. T., Guo, S., Zhong, L. J., Wiedensohler, A., and Zhang, Y. H.: Comparison of particle number size distributions and new particle formation between the urban and rural sites in the PRD region, China,

Atmos. Environ., 76, 181-188, doi:10.1016/j.atmosenv.2012.11.018, 2013.

Zhang, R.: Getting to the Critical Nucleus of Aerosol Formation, Science, 328, 1366-1367, 2010.

Zhang, R., Khalizov, A., Wang, L., Hu, M., and Xu, W.: Nucleation and growth of nanoparticles in the atmosphere, Chem. Rev., 112, 1957-2011, doi:10.1021/cr2001756, 2012.

Zhang, Y. M., Zhang, X. Y., Sun, J. Y., Lin, W. L., Gong, S. L., Shen, X. J., and Yang, S.: Characterization of new particle and secondary aerosol formation during summertime in Beijing, China, Tellus B, 63, 382-394, doi:10.1111/j.1600-0889.2011.00533.x, 2011.

Zhu, Y., Sabaliauskas, K., Liu, X., Meng, H., Gao, H., Jeong, C.-H., Evans, G. J., and Yao, X.: Comparative analysis of new particle formation events in less and severely polluted urban atmosphere, Atmos. Environ., 98, 655-664, doi:10.1016/j.atmosenv.2014.09.043, 2014.

Atmos. Chem. Phys. Discuss., doi:10.5194/acp-2016-806, 2016
Manuscript under review for journal Atmos. Chem. Phys.
Published: 24 October 2016

Atmospheric Chemistry and Physics Discussions

Figure and Table captions

Fig. 1. Relationship between sulfur dioxide concentration and condensation sink, and the data are 1 hour average values between 07:00 and 11:00 LT during NPF days (red) and non-NPF days (violet). Several remarkably high points were excluded.

Fig. 2. The particle number concentration of 3-6 nm (blue) and sulfuric acid concentration (red) on 15 October 2014, fitting as a power of 1.75 with the Pearson's R^2 of 0.622

Fig. 3. Time series during 31 October-9 December 2014 and the shaded areas are NPF days: (a) contour plot of particle number size distribution using NAIS data; (b) sulfur dioxide (blue) and ozone (red); (c) meteorological parameters, including wind speed (cyan), wind direction (green), temperature (magenta) and relative humidity (earth yellow).

Fig. 4. Wind rose plots of all NPF days (a) and non-NPF days (b), and data include the wind speed and wind direction between 07:00 and 11:00 LT. Length of each spoke on the circle represents the probability of wind coming from a particular direction at certain ranges of wind speed.

Fig. 5. Left panel (a) is the air mass back trajectories of all NPF days at 6:00 LT at 1535 m ASL for 72 h, including four NPF haze days (magenta). Panels (b)-(e) are the air mass backward trajectories for 24 h at 4:00, 6:00, 8:00 and 10:00 LT on four NPF haze days, and the time difference between UTC and LT is 8 h.

Fig. 6. Growth rates (red) and $PM_{2.5}$ (violet) during 31 October-9 December 2014, length of the bars in red represents the value of growth rate and width is the duration of NPF events.

Fig. 7. NPF events on clean day (29 September 2014) and polluted day (8 November 2014), each NPF day includes contour plots using WPS instrument (a, f) and NAIS instrument (b, g), time series of nucleation particle concentration and geometric median diameter (c, h), stack columns of particle number concentration (d, i) and volume concentration (e, j), and $PM_{2.5}$ variation (e, j). Missing parts of WPS on 8 November after 18:30 LT was for instrument maintaining.

Fig. 8. Diurnal variation of particle number concentration in 2 nm, 3 nm, 20 nm and 40 nm on 18 October 2014 (NPF, haze day, olive), 17 November 2014 (NPF, non-haze day, red) and 20 November 2014 (non-NPF, haze day, violet)

Table 1. Calculated parameters of all NPF events during three campaigns

Table 2. Summary of mean, median, 25th percentile, 75th percentile, minimum and maximum for calculated parameters

Table 3. The NPF characteristics comparison between Mt. Tai and other typical researches in China

Atmos. Chem. Phys. Discuss., doi:10.5194/acp-2016-806, 2016
Manuscript under review for journal Atmos. Chem. Phys.
Published: 24 October 2016

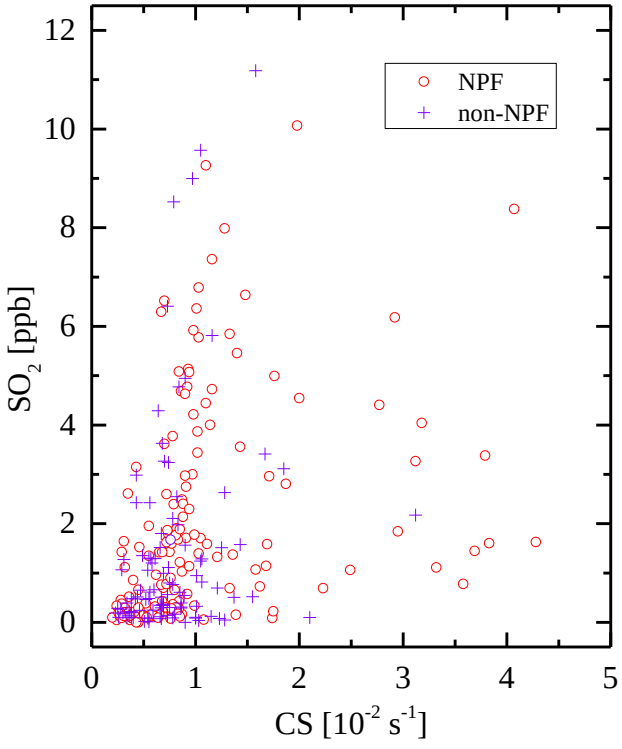

Fig. 1. Relationship between sulfur dioxide concentration and condensation sink, and the data are 1 hour average values between 07:00 and 11:00 LT during NPF days (red) and non-NPF days (violet). Several remarkably high points were excluded.

Atmos. Chem. Phys. Discuss., doi:10.5194/acp-2016-806, 2016
Manuscript under review for journal Atmos. Chem. Phys.
Published: 24 October 2016

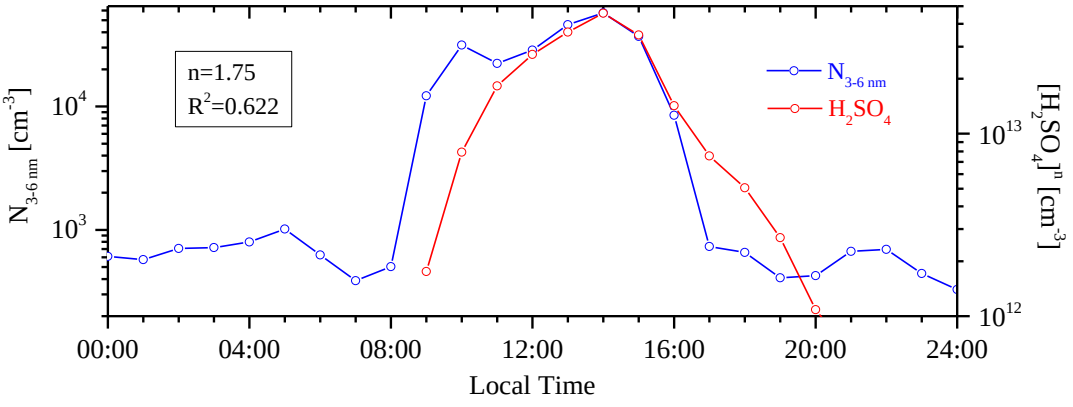

Fig. 2. The particle number concentration of 3-6 nm (blue) and sulfuric acid concentration (red) on 15 October 2014, fitting as a power of 1.75 with the Pearson's R^2 of 0.622

Atmos. Chem. Phys. Discuss., doi:10.5194/acp-2016-806, 2016
Manuscript under review for journal Atmos. Chem. Phys.
Published: 24 October 2016

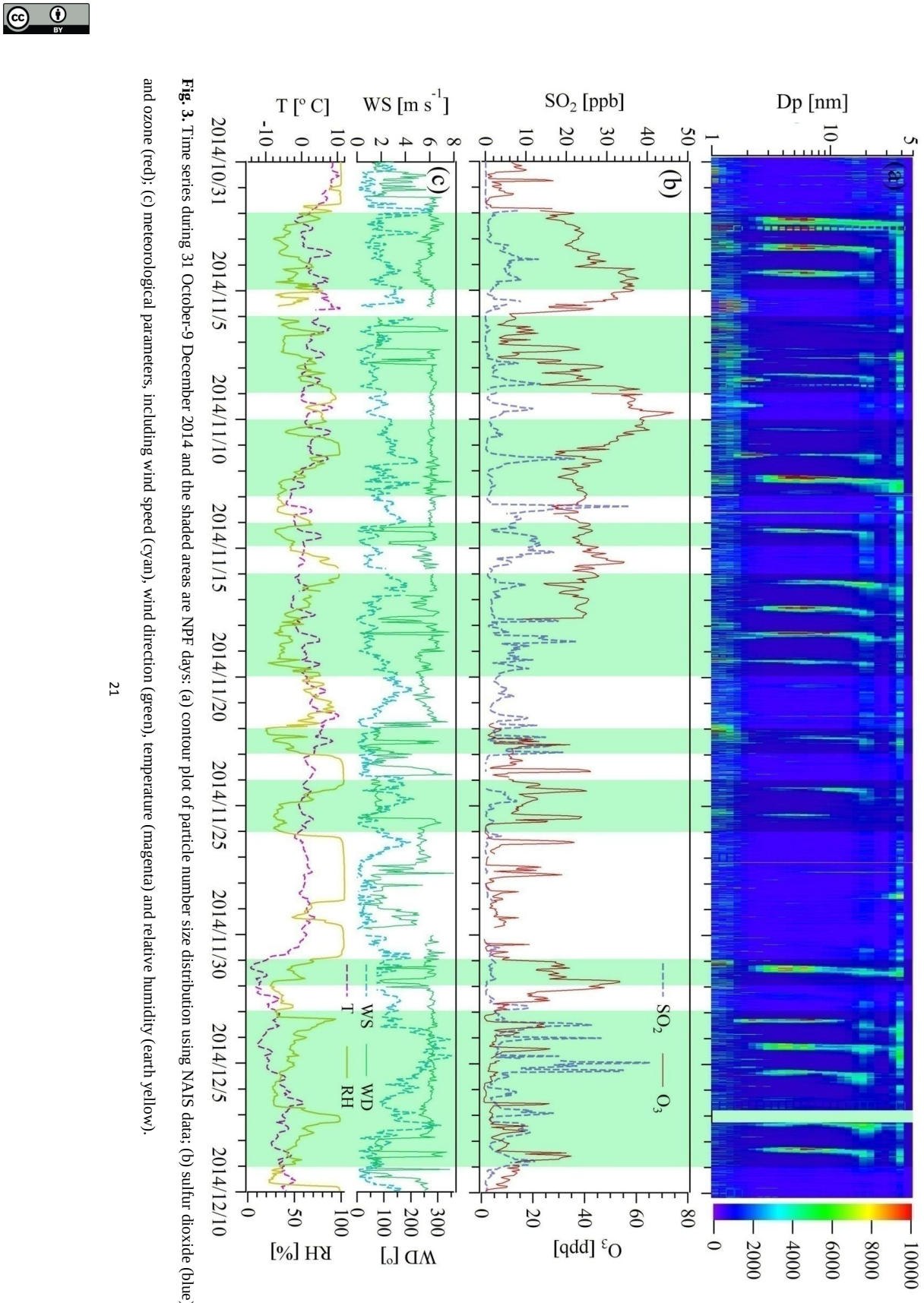

Fig. 3. Time series during 31 October-9 December 2014 and the shaded areas are NPF days: (a) contour plot of particle number size distribution using NAIS data; (b) sulfur dioxide (blue) and ozone (red); (c) meteorological parameters, including wind speed (cyan), wind direction (green), temperature (magenta) and relative humidity (earth yellow).

Atmos. Chem. Phys. Discuss., doi:10.5194/acp-2016-806, 2016
Manuscript under review for journal Atmos. Chem. Phys.
Published: 24 October 2016

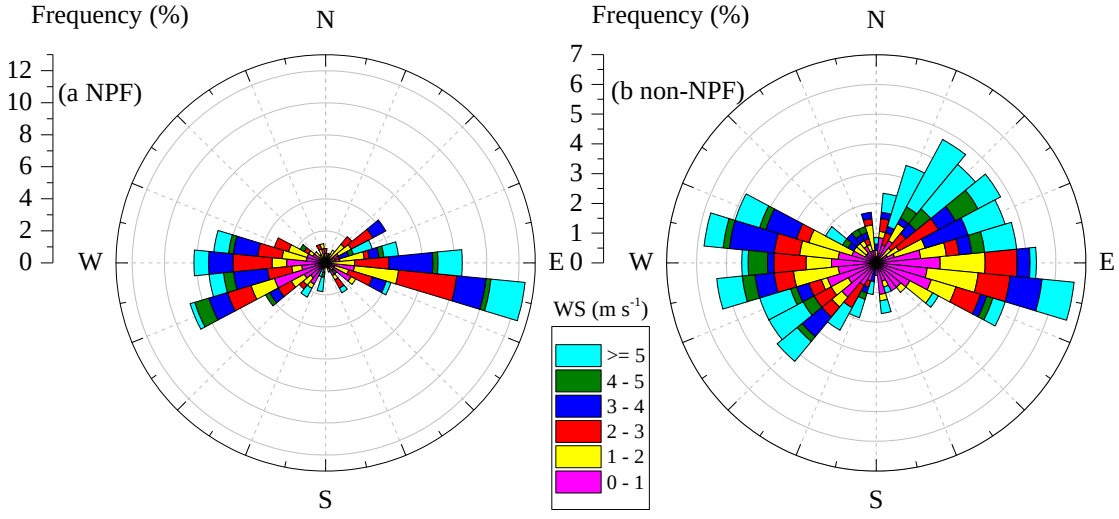

Fig. 4. Wind rose plots of all NPF days (a) and non-NPF days (b), and data include the wind speed and wind direction between 07:00 and 11:00 LT. Length of each spoke on the circle represents the probability of wind coming from a particular direction at certain ranges of wind speed.

Atmospheric Chemistry and Physics Discussions
Atmos. Chem. Phys. Discuss., doi:10.5194/acp-2016-806, 2016
Manuscript under review for journal Atmos. Chem. Phys.
Published: 24 October 2016

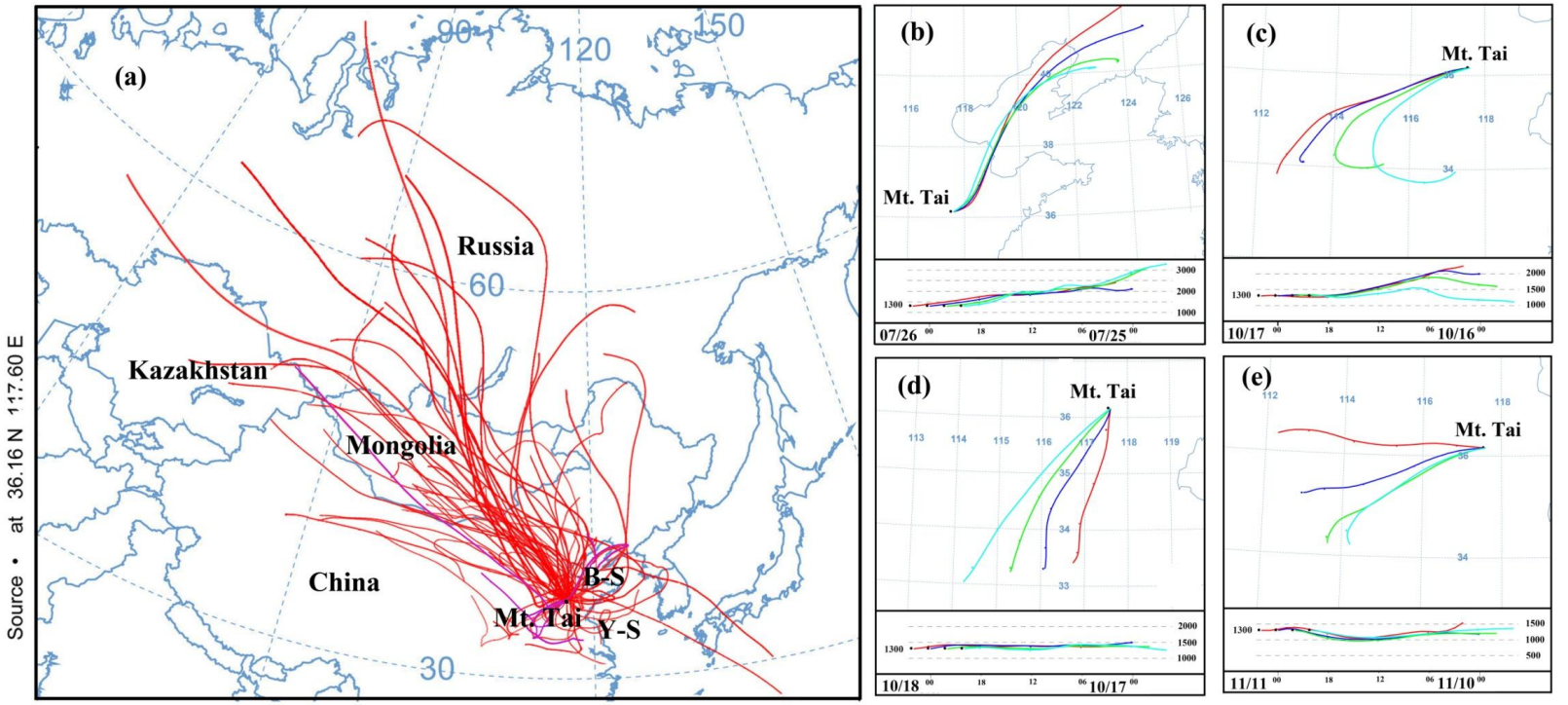

Fig. 5. Left panel (a) is the air mass back trajectories of all NPF days at 6:00 LT at 1535 m ASL for 72 h, including four NPF haze days (magenta). Panels (b)-(e) are the air mass backward trajectories for 24 h at 4:00, 6:00, 8:00 and 10:00 LT on four NPF haze days, and the time difference between UTC and LT is 8 h.

Atmos. Chem. Phys. Discuss., doi:10.5194/acp-2016-806, 2016
Manuscript under review for journal Atmos. Chem. Phys.
Published: 24 October 2016

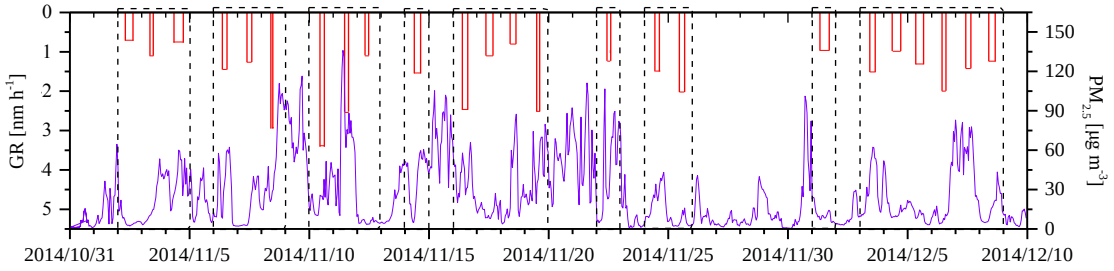

Fig. 6. Growth rates (red) and $PM_{2.5}$ (violet) during 31 October-9 December 2014, length of the bars in red represents the value of growth rate and width is the duration of NPF events.

Atmos. Chem. Phys. Discuss., doi:10.5194/acp-2016-806, 2016
Manuscript under review for journal Atmos. Chem. Phys.
Published: 24 October 2016

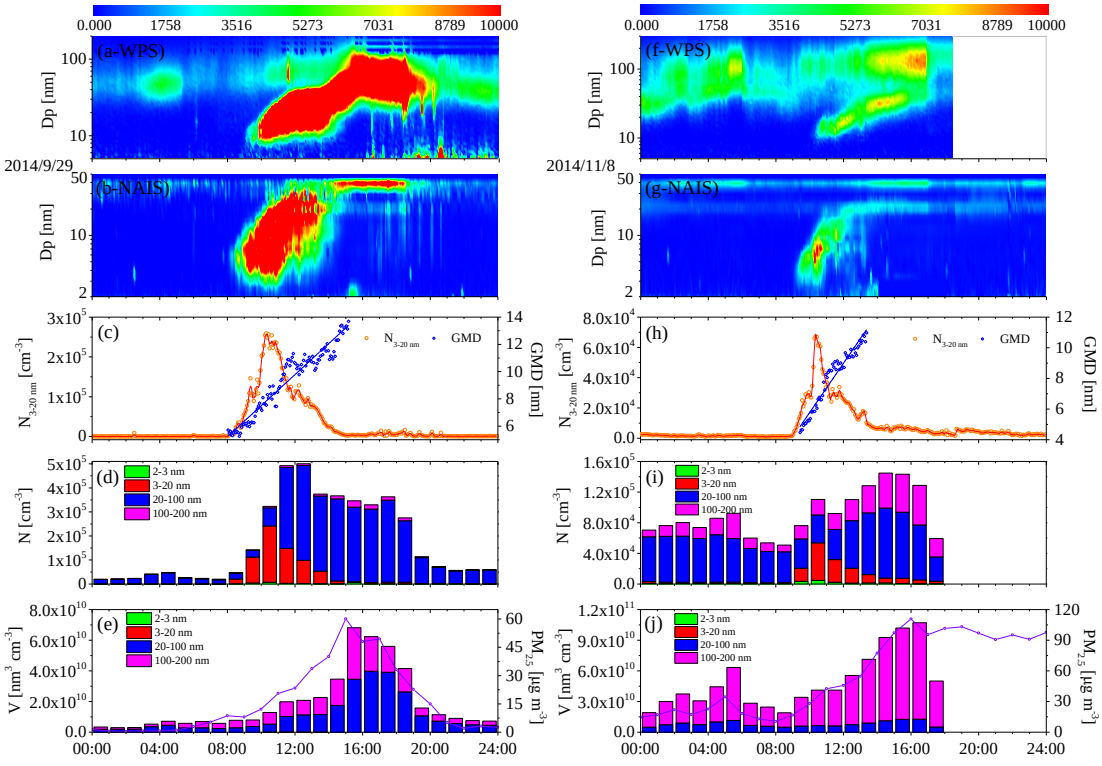

Fig. 7. NPF events on clean day (29 September 2014) and polluted day (8 November 2014), each NPF day includes contour plots using WPS instrument (a, f) and NAIS instrument (b, g), time series of nucleation particle concentration and geometric median diameter (c, h), stack columns of particle number concentration (d, i) and volume concentration (e, j), and $PM_{2.5}$ variation (e, j). Missing parts of WPS on 8 November after 18:30 LT was for instrument maintaining.

Atmos. Chem. Phys. Discuss., doi:10.5194/acp-2016-806, 2016
Manuscript under review for journal Atmos. Chem. Phys.
Published: 24 October 2016

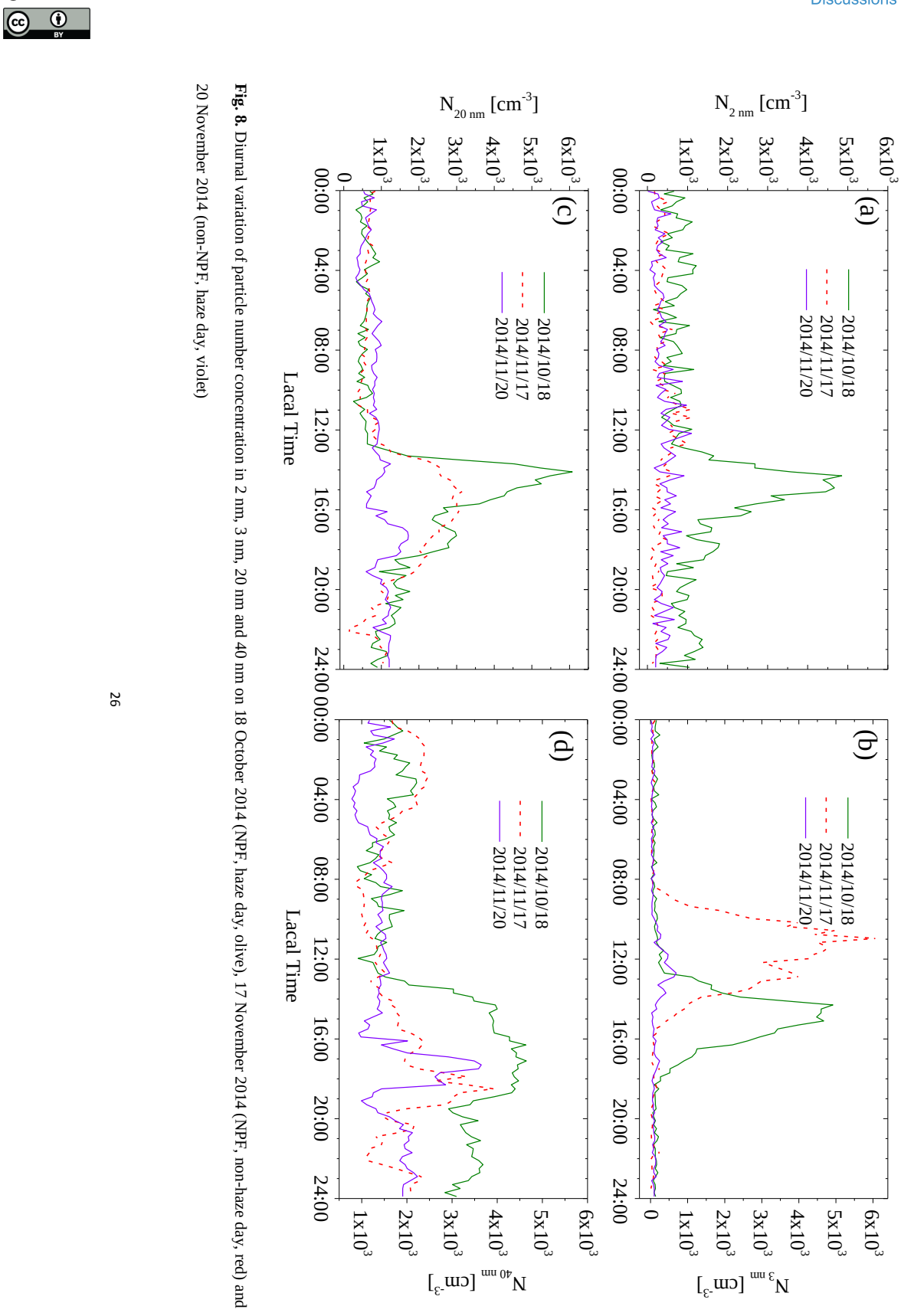

Fig. 8. Diurnal variation of particle number concentration in 2 nm, 3 nm, 20 nm and 40 nm on 18 October 2014 (NPF, haze day, olive), 17 November 2014 (NPF, non-haze day, red) and 20 November 2014 (non-NPF, haze day, violet)

Atmospheric Chemistry and Physics Discussions
Open Access

Table 1. Calculated parameters of all NPF events during three campaigns

Campaign	Date	$dN_{3\text{-}20}/dt$	$J_{3\text{-}20}$	GR	CS	SO_2	$[H_2SO_4]$	GR-C	GR-C/GR	Date	$dN_{3\text{-}20}/dt$	$J_{3\text{-}20}$	GR	CS	SO_2	$[H_2SO_4]$	GR-C	GR-C/GR
		$cm^{-3}\ s^{-1}$	$cm^{-3}\ s^{-1}$	$nm\ h^{-1}$	$10^{-2}\ s^{-1}$	ppb	$10^6\ cm^{-3}$	$nm\ h^{-1}$	%		$cm^{-3}\ s^{-1}$	$cm^{-3}\ s^{-1}$	$nm\ h^{-1}$	$10^{-2}\ s^{-1}$	ppb	$10^6\ cm^{-3}$	$nm\ h^{-1}$	%
I	26-Jul-14	8.96	13.32	1.54	3.59	4.27	1.95	0.09	5.92	8-Aug-14	10.67	16.30	1.15	2.62	2.98	**0.56**	**0.03**	2.28
	27-Jul-14	4.17	6.12	1.55	3.32	3.57	24.10	1.13	**72.66**	11-Aug-14	1.30	1.44	1.71	1.40	1.89	8.70	0.41	23.77
	2-Aug-14	3.23	3.60	3.81	2.01	N/A	1.96	0.09	2.40	12-Aug-14	28.84	40.13	3.69	4.04	12.9	5.08	0.24	6.43
	3-Aug-14	1.64	1.69	**7.76**	1.29	0.47	1.01	0.05	**0.61**	15-Aug-14	4.37	4.52	3.00	1.18	1.72	7.30	0.34	11.37
	6-Aug-14	37.74	52.54	5.78	1.99	N/A	3.08	0.14	2.49	20-Aug-14	1.21	1.33	4.80	1.93	8.18	9.19	0.43	8.95
	7-Aug-14	8.87	10.90	1.45	2.38	3.14	4.63	0.22	14.92									
II	22-Sep-14	1.20	1.58	1.12	6.08	5.89	8.26	0.39	34.46	4-Nov-14	10.67	15.06	0.77	1.73	6.48	2.69	0.13	16.32
	29-Sep-14	30.77	54.97	1.13	2.81	2.11	3.46	0.16	14.31	6-Nov-14	**0.96**	**1.10**	1.45	0.72	0.69	1.45	0.07	4.67
	30-Sep-14	15.51	20.61	1.62	1.79	2.46	1.17	0.05	3.37	7-Nov-14	5.50	5.59	1.26	**0.40**	0.45	1.53	0.07	5.67
	2-Oct-14	9.42	12.02	1.15	1.50	2.76	5.57	0.26	22.63	8-Nov-14	12.37	13.53	2.95	1.17	3.77	3.87	0.18	6.13
	3-Oct-14	8.63	14.07	1.50	2.27	2.07	3.98	0.19	12.40	10-Nov-14	2.07	2.17	3.41	0.55	3.02	1.50	0.07	2.06
	5-Oct-14	20.60	26.41	2.00	**6.32**	**0.18**	3.09	0.14	7.22	11-Nov-14	12.80	14.42	2.52	2.27	15.8	14.80	0.69	27.44
	6-Oct-14	8.54	8.94	0.78	2.12	0.34	0.87	0.04	5.21	12-Nov-14	11.67	26.36	1.09	2.14	1.62	N/A	N/A	N/A
	8-Oct-14	1.17	1.40	0.92	1.68	5.23	11.00	0.51	55.87	14-Nov-14	11.33	13.41	1.55	1.26	9.65	4.37	0.20	13.17
	10-Oct-14	21.45	27.04	1.80	1.19	3.62	8.05	0.38	20.90	16-Nov-14	10.55	11.06	2.47	2.03	7.05	6.03	0.28	11.41
	11-Oct-14	9.59	20.37	0.70	4.23	5.61	6.39	0.30	42.66	17-Nov-14	10.58	16.82	1.10	1.49	1.62	4.17	0.19	17.71
	13-Oct-14	21.20	26.84	1.64	2.56	5.24	1.13	0.05	3.22	18-Nov-14	40.00	57.11	0.80	2.80	14.5	6.90	0.32	40.30
	14-Oct-14	13.79	18.11	1.55	1.69	6.38	N/A	N/A	N/A	19-Nov-14	12.19	15.41	2.51	1.29	7.48	6.26	0.29	11.65
	15-Oct-14	20.86	30.54	2.76	2.59	10.3	4.97	0.23	8.41	22-Nov-14	11.28	11.60	1.23	1.26	4.22	5.09	0.24	19.34
	16-Oct-14	22.53	36.96	**0.58**	1.91	3.37	1.30	0.06	10.47	24-Nov-14	22.00	24.51	1.50	1.26	4.53	8.57	0.40	26.70
	17-Oct-14	2.13	2.58	2.12	1.70	N/A	1.30	0.06	2.87	25-Nov-14	9.49	10.97	2.02	0.80	1.17	0.95	0.04	2.20
	18-Oct-14	17.70	22.89	2.03	2.88	N/A	4.37	0.20	10.06	1-Dec-14	5.51	7.55	1.77	1.38	1.58	N/A	N/A	N/A
	21-Oct-14	1.61	1.98	2.36	1.50	0.61	5.60	0.26	11.09	3-Dec-14	**48.52**	**57.43**	1.51	1.71	**17.5**	1.96	0.09	6.07
	24-Oct-14	8.24	8.99	1.25	1.10	0.66	N/A	N/A	N/A	4-Dec-14	8.16	10.62	2.69	1.62	2.96	2.69	0.13	12.83
	25-Oct-14	14.12	14.74	1.60	1.17	0.89	1.11	0.05	3.24	5-Dec-14	4.54	5.83	1.32	1.05	4.56	6.54	0.31	23.15
	27-Oct-14	7.70	15.49	0.99	2.23	0.58	0.89	0.04	4.20	6-Dec-14	1.44	1.52	1.99	0.76	2.36	5.34	0.25	12.54
	28-Oct-14	11.59	13.17	1.21	1.11	0.37	5.32	0.25	20.55	7-Dec-14	7.78	11.64	1.42	2.41	9.37	3.63	0.17	11.95
	2-Nov-14	9.91	17.78	0.72	1.70	0.67	2.79	0.13	18.11	8-Dec-14	12.11	16.33	1.24	1.75	4.25	6.28	0.29	23.67
	3-Nov-14	10.82	18.57	1.10	2.19	4.88	5.80	0.27	24.64									
III	16-Jun-15	3.74	9.22	3.98	N/A	7.45	**25.40**	**1.19**	29.82	4-Jul-15	13.58	23.25	0.91	N/A	5.76	5.26	0.25	26.89
	20-Jun-15	18.20	32.50	3.28	N/A	4.34	9.52	0.44	13.56	8-Jul-15	4.44	8.25	0.93	N/A	1.71	9.72	0.45	48.63
	21-Jun-15	5.00	6.08	3.44	N/A	10.2	9.13	0.43	12.39	13-Jul-15	4.83	5.64	1.95	N/A	N/A	7.87	0.37	18.82
	2-Jul-15	14.10	43.41	1.08	N/A	3.92	10.30	0.48	44.73	15-Jul-15	14.33	19.72	2.86	N/A	N/A	1.82	0.09	2.97
	3-Jul-15	7.14	10.86	2.65	N/A	6.85	6.19	0.29	10.91	25-Jul-15	13.43	19.56	1.88	N/A	0.31	5.31	0.25	13.21

Atmos. Chem. Phys. Discuss., doi:10.5194/acp-2016-806, 2016
Manuscript under review for journal Atmos. Chem. Phys.
Published: 24 October 2016

Atmos. Chem. Phys. Discuss., doi:10.5194/acp-2016-806, 2016
Manuscript under review for journal Atmos. Chem. Phys.
Published: 24 October 2016

Atmospheric Chemistry and Physics Discussions

Table 2. Summary of mean, median, 25th percentile, 75th percentile, minimum and maximum for calculated parameters

	Mean	Minimum	Maximum	25th percentile	Median	75th percentile
$J_{3\text{-}20}$ (cm^{-3} s^{-1})	16.61	1.10	57.43	6.12	13.47	20.61
GR ($nm\ h^{-1}$)	1.98	0.58	7.76	1.15	1.55	2.51
CS (10^{-2} s^{-1})	2.00	0.40	6.32	1.26	1.72	2.33
[H_2SO_4] (10^6 cm^{-3})	5.47	0.56	25.40	1.96	5.03	6.90
GR-C ($nm\ h^{-1}$)	0.26	0.03	1.19	0.09	0.23	0.32
GR-C/GR (%)	16.20	0.61	72.66	5.92	12.40	22.63

Atmos. Chem. Phys. Discuss., doi:10.5194/acp-2016-806, 2016
Manuscript under review for journal Atmos. Chem. Phys.
Published: 24 October 2016

Atmospheric Chemistry and Physics Discussions

Table 3. The NPF characteristics comparison between Mt. Tai and other typical researches in China

Observation site	*J* cm^{-3} s^{-1}	GR nm h^{-1}	Frequency	Data	Air mass style	Ref.
Mt. Tai	16.61	1.98	40 %	Jul-Dec 2014 & Jun-Aug 2015	Mountain (1530 m ASL)	This study
Mt. Tai Mo Shan (Hong Kong)	2.94	3.86	33 %	Oct-Nov 2010	Mountain (640 m ASL)	Guo et al. (2012)
Mt. Huang (Anhui province)		3.58	18 %	Sep-Oct 2012	Mountain (869 m ASL)	Hao et al. (2015)
Mt. Daban (Qinghai province)		2.0	79 %	Sep-Oct 2013	Mountain (3295 m ASL)	Du et al. (2015)
SouthYellow Sea & East China Sea	4.3	6.3	16 %	Oct-Nov 2011 & Nov 2012	Marine	Liu et al. (2014)
Backgarden (Guangdong province)	3.4	12.1	25 %	Jul 2006	Rural	Yue et al. (2013)
Nanjing	2.6	10.4	44 %	Dec 2011-Nov 2013	Suburban	Qi et al. (2015)
Lanzhou		4.4	32 %	Jun-Jul 2006	Suburban	Gao et al. (2011)
Xinken (Guangdong province)	3.4	8.3	26 %	Oct-Nov 2004	Suburban	Liu et al. (2008)
Shanghai	8.7	11.4	21 %	Nov 2013-Jan 2014	Urban	Xiao et al. (2015)
Nanjing	3.7	7.6	40 %	Jul-Aug 2012	Urban	An et al. (2015)
Beijing	13.6	4.7	26 %	Jul-Sep 2008	Urban	Wang et al. (2015)
Guangzhou		14.5	9.5 %	Jul 2006	Urban	Yue et al. (2013)
Qingdao	13.3	6.2	41 %	Apr-May 2010	Urban	Zhu et al. (2014)
Hong Kong	1.9	5.2	23 %	Dec 2010-Jan 2011	Urban	Wang et al. (2014)